Ceramics International **21** (1995) 195–206

The Properties of Zirconia Powders Produced by Homogeneous Precipitation

B. Djuričić, S. Pickering, D. McGarry, P. Glaude, P. Tambuyser & K. Schuster

Institute for Advanced Materials, Commission of the European Communities, NL-1755 ZG Petten, The Netherlands

(Received 2 February 1994; accepted 7 March 1994)

Abstract: Spherical particles of zirconia were obtained by the calcination of monodisperse oxy-basic zirconium carbonate particles produced by homogeneous precipitation from zirconium sulphate solutions. By varying the salt concentration, monodisperse powders with diameters of 0·2–3 microns were obtained. The evolution of the structural characteristics of these powders during the calcination process was studied in some detail. The most interesting findings were the development of fully crystalline tetragonal zirconia at temperatures as low as 300°C and the existence of the metastable zirconia in domains of up to 100 nm in diameter. These domains appeared to exhibit a sub-structure of closely oriented nanocrystallites. By comparing powders calcined in air and nitrogen it appeared that the stability of the metastable tetragonal phase with respect to monoclinic zirconia was enhanced in sub-stoichiometric material. The interpretation of measurements of crystallite size and microstrain by X-ray diffraction is also discussed.

1 INTRODUCTION

The full technological potential of advanced zirconia ceramics will not be realized until microstructural defects can be eliminated.[1] The most serious microstructural defects are those packing heterogeneities introduced during powder processing which persist into the final microstructure.[2] Powder characteristics such as spherical particle shape and well-defined size help to reduce such heterogeneities by enhancing the powder flow and packing efficiency in green bodies. Powders with better processing characteristics are therefore expected to contribute to reducing microstructural heterogeneities, and various synthesis methods are being explored for their ability to deliver such powders.[2–10] However, because commercial production and processing techniques must be relatively simple and cheap, only a few of the laboratory methods can be seriously considered for industrial application. Homogeneous precipitation is one of these methods.

Homogeneous precipitation has long been of interest to chemists as a means of obtaining colloids of well-defined morphology and composition.[10–12] However, it is only recently that this technique has been applied to the preparation of ceramic powders.[12–16] The essential feature of homogeneous precipitation is that precipitation is brought about by a highly uniform increase in the pH of the solution, and that this uniformity is achieved by the thermal decomposition of urea. Thus, when an acidic solution of a metal salt, in which urea has been dissolved, is gently heated to about 85°C, the urea decomposes with the release of ammonium and carbonate ions into solution. The gradual and uniform rise in pH results in the nucleation and growth of uniformly sized and shaped particles of insoluble metal oxy-basic carbonate. The process is suitable for the synthesis of monodisperse spherical powders of a variety of oxide ceramics.

The chemical, structural and morphological characteristics of the precipitate particles depend primarily on the chemical species present and on their concentrations, but the particle characteristics also depend on other processing parameters, and the influence of some processing parameters on the particle properties may still be detected

Ceramics International 0272-8842/95/$9.50

after calcination of the precipitate to yield the final oxide powder. Whereas the influence of some process parameters is understood, others still remain to be elucidated. For example, the stability of the metastable tetragonal zirconia phase at low temperatures has been ascribed to factors as diverse as: a critical particle size effect,[17] the effect of anionic vacancies[18] and ionic impurities, e.g. the SO_4^{2-} group,[19] a structural similarity between amorphous precursor gels and tetragonal zirconia,[20,21] the effect of water vapour,[22] the presence of domain boundaries,[23] and the effect of the washing medium.[24] The relative importance of these mechanisms is not yet fully understood.

The fact that the properties of the ceramic powder depend relatively sensitively on various processing parameters means that the homogeneous precipitation process cannot be considered sufficiently mature for commercial exploitation until these dependencies are better understood. This paper tries to contribute to this understanding by exploring in depth the structural changes and phase evolution during the calcination of oxy-basic zirconium carbonate to form monodisperse spherical zirconia particles.

2 EXPERIMENTAL PROCEDURES

2.1 Materials

Zirconium sulphate tetrahydrate ($Zr(SO_4)_2 \cdot 4H_2O$) (Janssen Chemica, 99·99%); urea (CON_2H_4) (Janssen Chemica, high purity), Polyvinylpyrrolidone K-30 (Aldrich-Chemie, special grade); nitric acid (HNO_3) (J. T. Baker Chemicals, 'Baker Analyzed' reagent grade) were used as received.

2.2 Preparation of spherical precursor particles

Zirconium sulphate tetrahydrate was dissolved in de-ionized water and the pH of the solution was adjusted with diluted nitric acid to a value of about 2. Polyvinylpyrrolidone (PVP) and urea were dissolved in this solution. The stirred solution was heated to 85°C at a rate of about 2°C/min and held at this temperature for a further 180 minutes to decompose the urea[25] and induce precipitation of colloidal particles, and to allow their growth to micron-sized spheres. The dispersion was then cooled to room temperature with cold water and centrifuged at about 900 g for 20 min, the supernatant solution was discarded, and the particles were resuspended in de-ionized water in an ultrasonic bath to wash the precipitate. The pH of de-ionized water was adjusted to 9·5–10 using ammonium hydroxide to prevent dissolution of the particles. The washing process was repeated until sulphate ions were no longer detectable in the washing water (barium chloride test). The precipitate was then dispersed in isopropyl alcohol using an ultrasonic bath, centrifuged, and dried at 80–100°C overnight.

2.3 Calcination and characterization

Gram quantities of the dried precipitate were calcined at various temperatures, either in air or in nitrogen, to provide samples representing different stages in the conversion of the oxy-basic zirconium carbonate precursor material to zirconium oxide. The changes that occurred during calcination were also investigated using simultaneous thermogravimetric analysis (TGA) and differential thermal analysis (DTA) (NETSCH, Simultaneous Analyzer STA 409) to 1200°C. All calcinations and DTA analyses were made using a heating rate of 5°C/min, and a cooling rate of 2°C/min.

Scanning electron microscopy (SEM, Zeiss DSM 940) provided information on particle size and shape before and after calcination. The SEM samples were prepared by dispersing particles in ethyl alcohol in an ultrasonic bath for 2–3 min and allowing a drop of the resulting suspension to dry on a specimen holder. The calcined particles were examined by transmission electron microscopy, TEM, (Philips EM 400). The TEM samples were prepared by placing a drop of a suspension of particles in alcohol onto a carbon coated grid and allowing it to dry by evaporation.

X-ray diffraction (Philips PW173 X-ray diffractometer) was used to determine the phases present in the calcined powders and to estimate crystallite size. The percentages of the monoclinic and tetragonal phases were calculated from the integrated intensities of the monoclinic ($\bar{1}11$) and (111) peaks and from the tetragonal (111) peak.[26] To minimize the risk of mechanical induced formation of the monoclinic phase, the samples were not mechanically treated before XRD examination.

Crystallite size was estimated from the broadening of the X-ray diffraction peaks. However, two phenomena can contribute to peak broadening, namely, small crystallite size and microstrain (lattice disorder), and the separation of these two contributions is not always reliable. The Scherrer equation attributes all peak broadening to crystallite size:[27]

$$D_{app} = K\lambda/(B \cos \theta) \quad (1)$$

where D_{app} is the apparent crystallite size, λ is the wavelength of CuK_α radiation (1·5406 Å), B is the width of the peak (in radians) after correction for

instrumental broadening. The correction for instrumental peak broadening was made using the Warren formula: $B^2 = b^2_{ob} - b^2_{st}$, where b_{ob} and b_{st} are the peak widths at half peak height for zirconia and a LaB_6 standard, respectively. K is an empirical constant which we assumed = 1.[28] The peak widths were calculated using a Voigt peak fitting routine. The limitations of eqn (1) become apparent when D_{app} is calculated for different orders of the same hkl reflection, e.g. (111) and (222). Because these are measurements in the same direction, they should yield the same D_{app}. i.e.

$$D_{app} = \lambda/(B_1 \cos \theta_1) = \lambda/(B_2 \cos \theta_2) \quad (1a)$$

Equation (1a) therefore holds under the condition: $B_2 = B_1 \cos \theta_1/\cos \theta_2$. In practice this is not always the case, and it is customary to attribute any deviation from this condition to microstrain, and to modify eqn (1) accordingly, as in the Hall equation:

$$(B_{hkl} \cos \theta)/\lambda = 1/D_{hkl} + \eta_{hkl} (\sin \theta/\lambda) \quad (2)$$

which is applied to pairs of peaks of the same family such as $(111)_t/(222)_t$ where D_{hkl} denotes the effective crystallite size in the hkl direction and η_{hkl} the microstrain in that direction. Substituting in experimental values of B and θ for the two peaks, microstrain is calculated from:

$$\eta = (B_1 \cos \theta_1 - B_2 \cos \theta_2)/(\sin \theta_1 - \sin \theta_2) \quad (2a)$$

It is clear from these equations that microstrain is only a measure of the difference in broadening of the two diffraction peaks. Either positive or negative values may be obtained depending on whether B_2 is greater or less than $B_1 \cos \theta_1/\cos \theta_2$. Microstrain is therefore not interpreted only in terms of compressive and tensile stress fields in the usual macroscopic sense. Instead, the microstrain type of peak broadening can also be due to lattice disorder localized in a single plane resulting from a slight displacement of atoms from their equilibrium

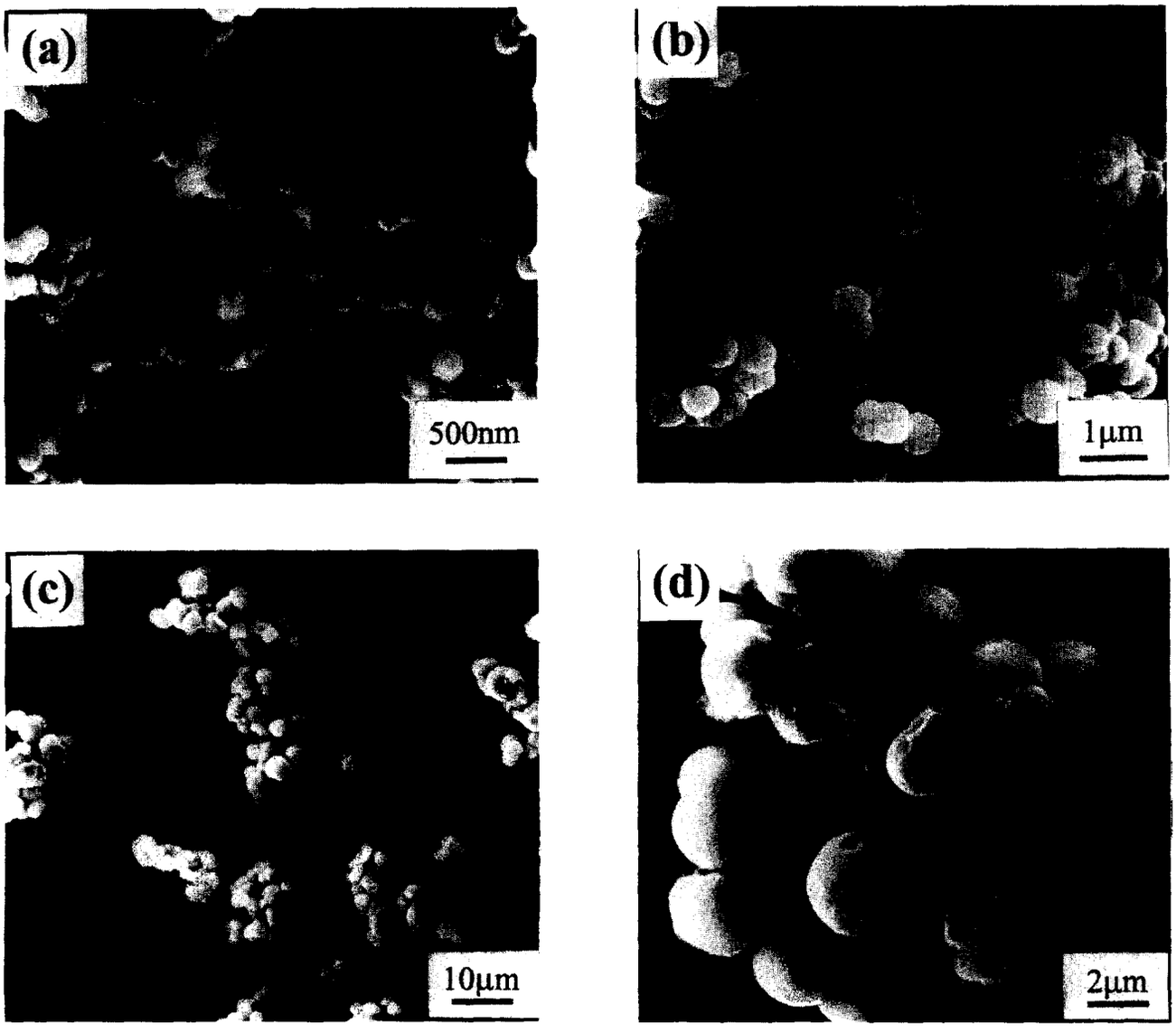

Fig. 1. SEM micrographs of zirconium oxy-basic carbonate particles produced from various concentrations of $Zr(SO_4)_2 \cdot 4H_2O$: (a) 5×10^{-3}, (b) 10^{-2}, (c) and (d) 5×10^{-2} mol/l.

Table 1. Conditions for the synthesis of zirconium oxy-basic carbonate particles

Concentration of reactants			Ageing temp. (°C)	Ageing time (min)	Final solution pH	Particle shape	Size distribution
$Zr(SO_4)_2 \cdot 4H_2O$ (mol/l)	Urea (mol/l)	PVP (wt%)					
5×10^{-3}	2	0·3	85	180	8·25	spherical	narrow
1×10^{-2}	2	0·3	85	180	8·38	spherical	narrow
5×10^{-2}	2	0·3	85	180	6·74	Irregular	broad

positions in a direction perpendicular to the lattice plane. Equation (2) attributes as much peak broadening to the effects of small crystallite size as is compatible with the condition $B_2 = B_1 \cos \theta_1 / \cos \theta_2$, i.e. it implicitly assumes that the lattice plane corresponding to peak 1 is completely free from lattice disorder. Consequently, if the lattice planes corresponding to peaks 1 and 2 both exhibit an equal and large amount of lattice disorder, then the condition $B_2 = B_1 \cos \theta_1 / \cos \theta_2$ is fulfilled and the calculated microstrain value is zero. The microstrain value is therefore a measure of the difference in lattice disorder between two planes of the same family rather than an absolute measure. Consequently, although the Hall equation can give a better estimation of size than the Scherrer equation, it can still severely underestimate the true crystallite size.

3 RESULTS

3.1 Synthesis of particles

Spherical particles of zirconium oxy-basic carbonate, $Zr_2O_2(OH)_2 \cdot CO_3 \cdot 2H_2O$, are shown in Fig. 1 and the compositions of the reactant solutions from which they were obtained are given in Table 1. The rise in the pH of the solution during ageing is shown in Fig. 2. The role of the PVP was to reduce the agglomeration of large particles, which ultimately limits the development of the monodisperse population of spheres. The morphology and other properties of the spherical particles were quite sensitive to experimental conditions, for example, particle size and particle size distribution depended strongly on the concentration of zirconium sulphate as shown in Fig. 1. According to Matijevic,[10-12] the formation of monodisperse particles is largely determined by the nucleation process, i.e. homogeneous nucleation results in a monodisperse sol with a number concentration of particles independent of the salt concentration: the role of the reactant concentration in homogeneous precipitation is to determine the maximum size to which the sol particles can subsequently grow. Figure 3 shows that the final size of the spherical particles increased with increasing concentration of zirconium sulphate.

The zirconium sulphate concentration of 5×10^{-2} mol/l appears to have been too high for the formation of well-defined monodisperse particles in these experiments. At this concentration, the final pH of the solution was very much lower than in other cases, the particles agglomerated to form assemblies of linked particles which settled rapidly from the mother solution, and the particle size

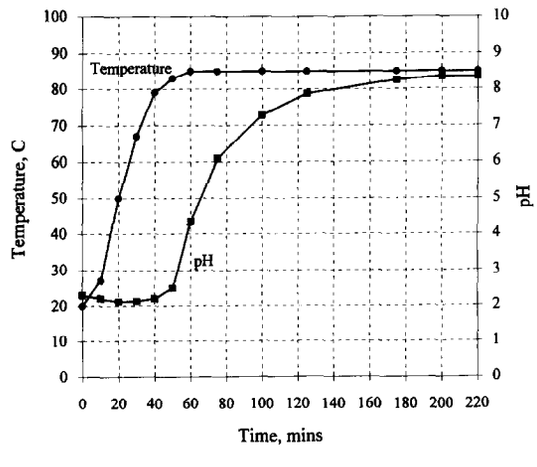

Fig. 2. Evolution of the pH of the solution during precipitation and growth of spherical zirconium oxy-basic carbonate particles.

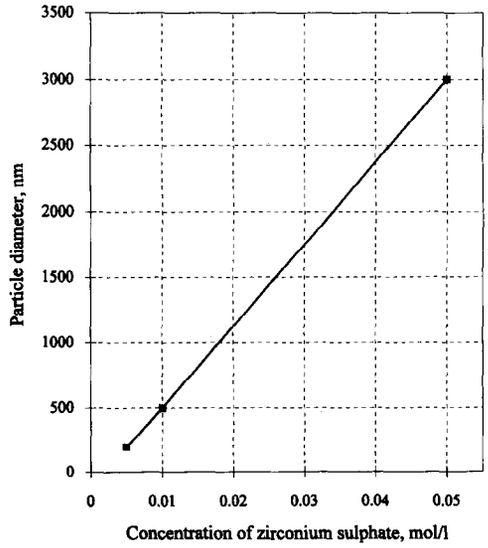

Fig. 3. Dependence of particle diameter on salt concentration.

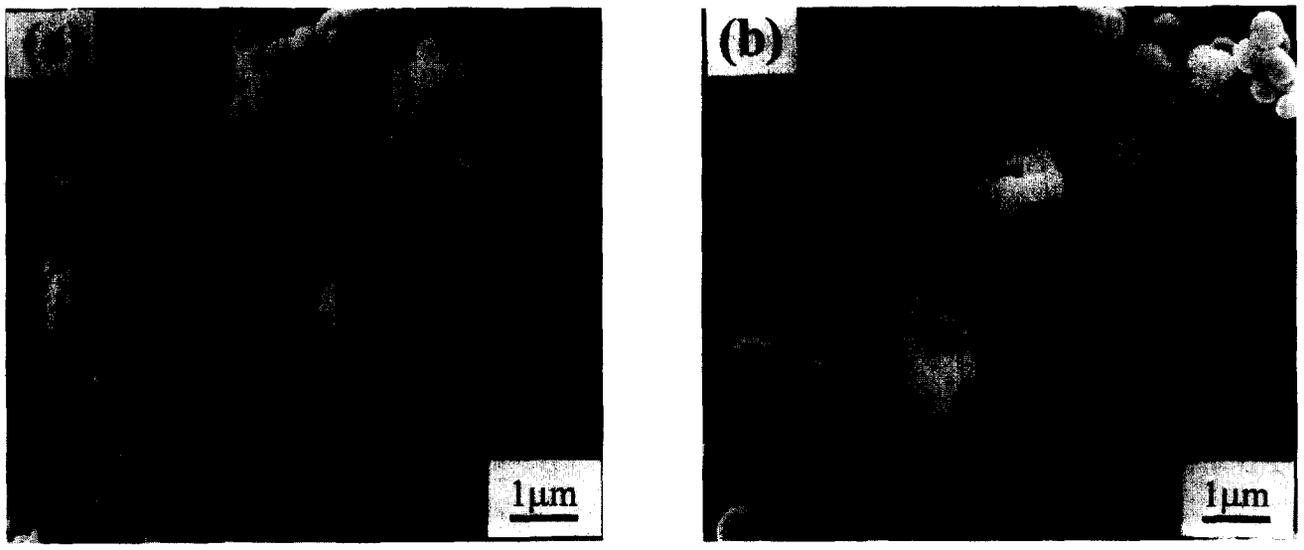

Fig. 4. SEM micrographs of zirconium oxy-basic carbonate particles: (a) after storage for 10 days in the mother solution (b) after calcination at 700°C for 1 h.

distribution broadened. Similar upper concentration limits for the reactants in homogeneous precipitation have been reported previously.[6]

At the lower salt concentrations, the pH of the reactant solution after ageing was about the same and a narrow particle size distribution was obtained. After ageing, these particles appeared to be stable in the mother solution at room temperature: no deterioration in sphericity could be observed after storage for 10 days (Fig. 4a). After drying, the particles were only weakly agglomerated and they could be easily redispersed by ultrasonification. Some shrinkage of the particles took place during calcination but the spherical shape was retained (Fig. 4b). Only particles produced from solutions with an initial concentration of 10^{-2} mol/l of zirconium sulphate were used for subsequent characterization as reported below.

3.2 Thermogravimetric analysis (TGA)

Particles produced from a solution concentration of 10^{-2} mol/l, as described above, were dried in air at 80°C for 16 h. Thermogravimetric analysis (TGA) on this material showed weight losses of about 20% on heating to 1200°C, both in air and in nitrogen, as shown in Fig. 5. These results are in good agreement[18] or are slightly lower[6,29] than the findings of other authors for similar precipitates. That lower weight losses have also been reported[30,31] may be attributed not only to differences in chemical composition, but also to differences in washing and drying procedures for the precipitate. Most of the weight loss occurred during heating to 400°C, with the maximum rate of loss occurring at 150°C in air and at 135°C in nitrogen. A feature observed only in material calcined in air was a small weight gain starting at about 600°C; this phenomenon was also observed by Livage *et al.*[20] and Torralvo *et al.*[32] who attributed it to the filling of oxygen vacancies. In our material the weight gain was equivalent to a change in stoichiometry from $ZrO_{1.945 \pm 0.01}$ to ZrO_2 and was accompanied by a change in colour from grey to pure white. For powder calcined in nitrogen, in contrast, this mechanism would not be expected to occur, and we found no evidence for such a change: there was no increase in weight, nor did the powder become white at comparable or higher temperatures.

3.3 Differential thermal analysis (DTA)

DTA curves measured in flowing air and nitrogen are illustrated in Fig. 6. Broad endothermic peaks were observed at about 150°C which correspond to the volatilisation of water[29,30] and to carbonate decomposition;[29,33] these peaks coincide with substantial loss of weight as mentioned above. The

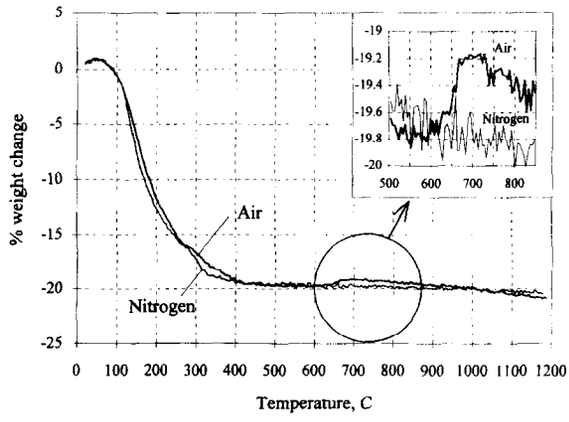

Fig. 5. Thermogravimetric analysis of zirconium oxy-basic carbonate.

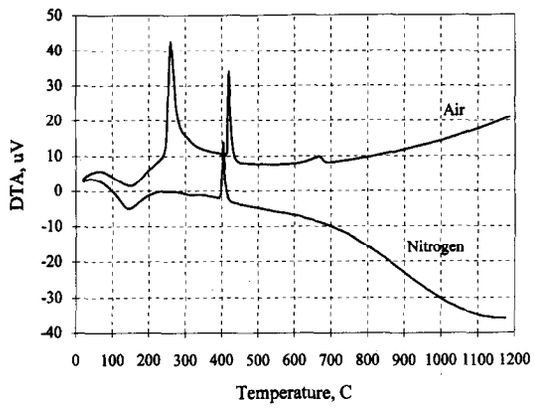

Fig. 6. Differential thermal analysis of zirconium oxy-basic carbonate.

narrow, well-defined exothermic peak at about 260°C on the DTA curves obtained in air is attributed to the oxidation of organic residues. According to XRD there was no phase change associated with this peak, and the peak was absent on DTA curves obtained in nitrogen. Similar exothermic peaks have been reported for precipitates which were in contact with organic materials at some stage during their preparation, but not for precipitates that have no history of contact with organics. For example, exothermic peaks have been reported: at about 310°C for a precipitate washed in ethanol,[24] at about 370°C for zirconia powders treated with ethanol,[34] and at 270°C for a precipitate produced by hydrolysis of $Zr(OC_3H_7)_4$ in isopropyl alcohol.[35] This latter value of 270°C corresponds closely to our value of 260°C for powder which was washed with isopropyl alcohol. In contrast, no comparable exothermic peaks have been reported for material produced by precipitation from zirconium salt with ammonia and washed with water.[20,29–31] A well-defined exothermic process was found to occur at 406°C in nitrogen and at 420°C in air. Previous authors have found similar exothermic peaks in this temperature range and refer to them as 'glow exotherms' which they attributed to a release of bound hydroxyl groups and crystallization. However, as will be discussed later, our results differ from previous findings in some important respects.

Thermal treatment changed the colour of the powders as shown in Table 2. Above the 'glow exotherm' temperature, powder calcined in nitrogen was darker grey than that calcined in air. We attribute the grey colour to oxygen vacancies. At higher temperatures, e.g. 700°C, powders calcined in air were pure white, indicating that the oxygen vacancies had been filled, but powders calcined in nitrogen remained grey up to 1200°C, which was the highest temperature used in this work.

The filling of oxygen vacancies should result in a weight gain and such a weight gain was indeed recorded by TGA in the temperature range 600–680°C. Moreover, DTA revealed that this was an exothermic process. In contrast, neither the weight gain nor the exothermic process were observed in powders calcined in nitrogen. In air, cooling from 1200°C to room temperature revealed a weak exothermic peak at about 792°C which is associated with a phase transformation from tetragonal to monoclinic. In nitrogen, although there was no corresponding peak on the DTA cooling curve, the material was monoclinic at room temperature, indicating that the t → m transformation occurred over a wide temperature range. It has been noted earlier by Turrillas *et al.*[36] and Srinivasan *et al.*[37] the t → m phase transformation peak on cooling depends on factors such as precipitation and thermal treatment conditions.

3.4 X-ray diffraction analysis (XRD)

X-ray spectra for the precipitate calcined at temperatures up to 300°C are shown in Fig. 7. The spectrum is initially typical of that for a gel: the tail at diffraction angles below 10° indicates very small particles, and the broad bands, e.g. at about 30°, indicate an essentially amorphous precipitate with some nearest-neighbour ordering. At 250°C, after loss of water, organic residues, carbonate decomposition, etc., the broad peaks narrowed somewhat, indicating a slight increase in short-range ordering. At 300°C the main peak in the spectrum for the tetragonal phase, (111), appeared within the major broad peak in a manner analogous to the development of cristobalite from silica gel. The development of this tetragonal phase at 300°C was observed both in air and in nitrogen. The formation of this phase therefore does not appear to be associated with the exothermic peak at 260°C, which was observed only in air. Figure 7

Table 2. Colour of zirconia calcined for 1 h at various temperatures in air and nitrogen

Gas	Calcination temperature (°C)									
	100	250	300	380	500	600	700	750	800	1200
Air	white	ivory	ivory	lt grey	lt grey	grey	white	white	white	white
N_2	white	white	ivory	ivory	grey	grey	grey	grey	grey	grey

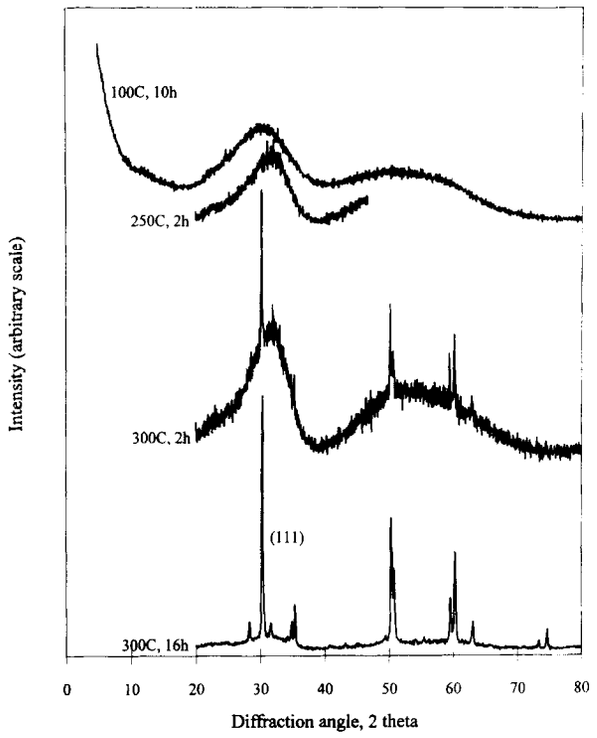

Fig. 7. X-ray spectra of zirconium oxy-basic carbonate after calcination at various temperatures.

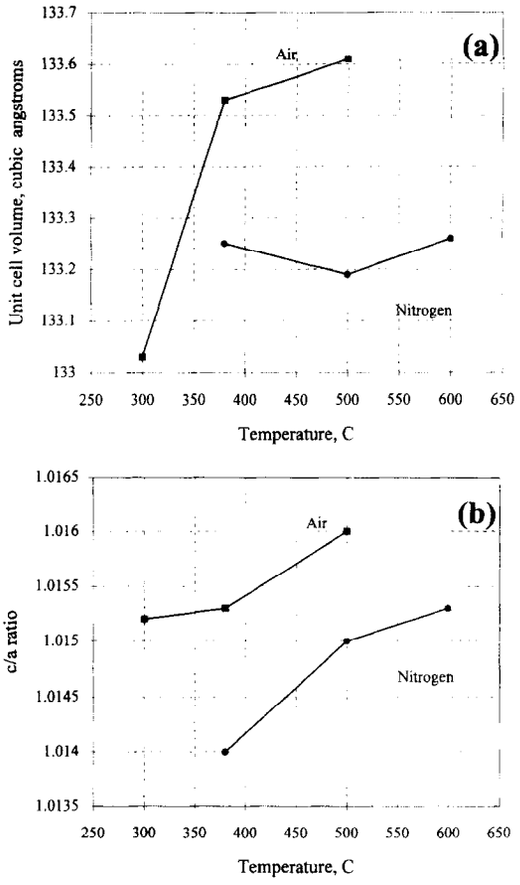

Fig. 8. Dependence on temperature of: (a) the unit cell volume and, (b) the *c*/*a* ratio, in zirconia calcined in air and nitrogen.

also indicates that the kinetics of formation of this tetragonal phase at 300°C. were rather slow so that crystallization of the tetragonal phase would be unlikely to correspond to a well-defined DTA peak at that temperature. The lattice parameters of the tetragonal phase after calcination of the powder for 1 h at various temperatures revealed significant differences between air and nitrogen atmospheres (Fig. 8).

At about 600°C in air and 750°C in nitrogen, the tetragonal phase transformed to monoclinic. Details of the phase composition are given in Fig. 9. The apparent and effective crystallite sizes, and microstrain, are shown in Tables 3, 4 and 5, respectively.

The effective crystallite sizes of the tetragonal phase shown in Table 4 are considerably larger than the maximum size previously reported[17,21–23,37] suggesting that the microtexture of zirconia prepared by homogeneous precipitation differs from that produced by other methods. Microstrain in the tetragonal phase is evidently higher after calcination in air than in nitrogen.

3.5 TEM examination

TEM images of the internal structure of spherical particles of up to 1 μm diameter were obtained

Table 3. Apparent crystallite sizes (nm) calculated from the Scherrer formula

Gas	Temp. (°C)	Tetragonal						Monoclinic							
		(111)	(222)	(002)	(004)	(200)	(400)	($\bar{1}$11)	($\bar{2}$22)	(002)	(003)	(110)	(220)	(011)	(022)
Air	300	40	35	36	51	46	47	—	—	—	—	—	—	—	—
	380	49	32	57	39	72	53	—	—	—	—	—	—	—	—
	500	43	42	34	24	47	34	—	—	—	—	—	—	—	—
	600	—	—	—	—	—	—	32	38	38	31	33	35	46	34
	700	—	—	—	—	—	—	54	38	44	37	42	45	55	46
	800	—	—	—	—	—	—	57	39	43	38	46	49	56	52
N_2	380	65	54	—	46	—	57	—	—	—	—	—	—	—	—
	500	52	47	—	—	—	—	—	—	—	—	—	—	—	—
	600	65	54	70	47	81	77	—	—	—	—	—	—	—	—
	750	49	—	—	—	—	—	45	41	—	—	—	—	—	—
	1200	—	—	—	—	—	—	44	32	—	—	—	—	—	—

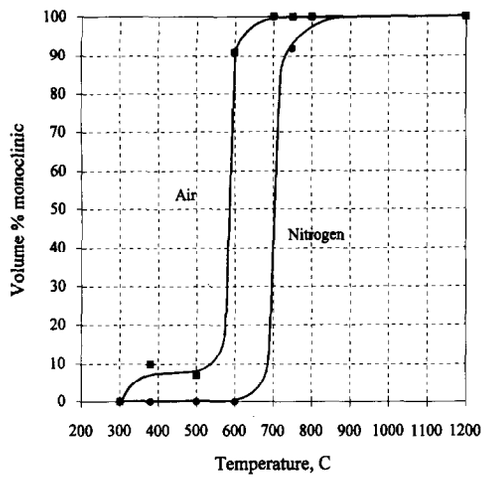

Fig. 9. Comparison of the dependence on temperature of the phase composition of zirconia calcined in air and nitrogen.

without difficulty. The transparency to the electron beam of such large particles indicates that the particles were highly porous. The TEM images showed that the development of a tetragonal crystal structure within the spherical particles, as evidenced by X-ray and electron diffraction for calcination temperatures above 300°C, was associated with the appearance of domain structures (Fig. 10). Domain boundaries were found in most spherical particles larger than about 200 nm: particles of 200 nm, however, usually contained only one domain (Fig. 11). In cases where spheres were in close contact during calcination, domains were also found extending over more than one particle, particularly for powders calcined in nitrogen (Fig. 12). Each domain gave an essentially 'single crystal' type electron diffraction pattern, but the spots were somewhat diffuse both for the tetragonal (Fig. 10) and monoclinic (Fig. 13) phases. Single domain particles of tetragonal zirconia transformed to single domain particles of monoclinic zirconia (Fig. 13), and polydomain particles of tetragonal zirconia transformed to polydomain particles of monoclinic zirconia, which, after calcination at 1000°C, were usually twinned (Fig. 14).

4 DISCUSSION

Monodisperse spherical particles were obtained by ageing of solutions containing urea. In this process, homogeneous nucleation is believed to be responsible for the development of the monodisperse size distribution. There are a number of

Table 4. Effective crystallite size (nm) for various families of crystallographic planes

Gas	Temp. (°C)	Tetragonal			Monoclinic			
		{111}	{002}	{200}	{$\bar{1}$11}	{002}	{110}	{011}
Air	300	46	27	46	—	—	—	—
	380	101	108	114	—	—	—	—
	500	101	62	75	—	—	—	—
	600	—	—	—	27	77	30	70
	700	—	—	—	91	66	39	68
	800	—	—	—	109	57	43	62
N_2	380	81			—	—	—	—
	500	60			—	—	—	—
	600	83	136	87	—	—	—	—
	750	—	—	—	49	—	—	—
	1200	—	—	—	66	—	—	—

Table 5. Microstrain in various families of crystallographic planes

Gas	Temp. (°C)	Tetragonal			Monoclinic			
		{111}	{002}	{200}	{$\bar{1}$11}	{002}	{110}	{011}
Air	300	0·0020	−0·0043	−0·0001	—	—	—	—
	380	0·0062	0·0043	0·0026	—	—	—	—
	500	0·0041	0·0067	0·0041	—	—	—	—
	600	—	—	—	−0·0033	0·0066	−0·0016	0·0056
	700	—	—	—	0·0048	0·0039	−0·0012	0·0025
	800	—	—	—	0·0052	0·0029	−0·0010	0·0012
N_2	380	0·0018	—	—	—	—	—	—
	500	0·0014	—	—	—	—	—	—
	600	0·0019	0·0035	0·0004	—	—	—	—
	750	—	—	—	0·0012	—	—	—
	1200	—	—	—	0·0049	—	—	—

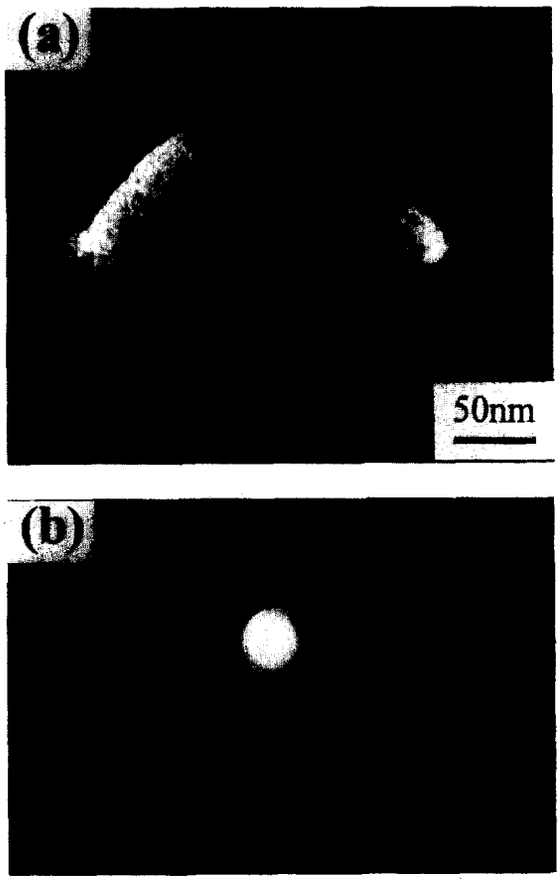

Fig. 10. TEM micrographs showing several domains in a particle of tetragonal zirconia after calcination for 1 h at 500°C in air: (a) dark field image corresponding to the (220) spot, (b) diffraction pattern showing diffuse spots.

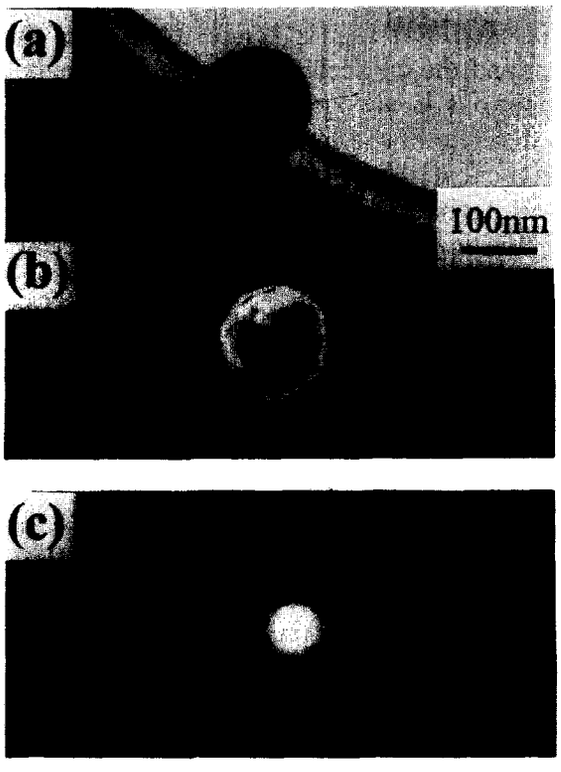

Fig. 11. TEM micrographs of a single domain monoclinic zirconia particle calcined at 700°C in air for 1 h: (a) bright field, (b) dark field corresponding to the (220) spot, (c) diffraction pattern.

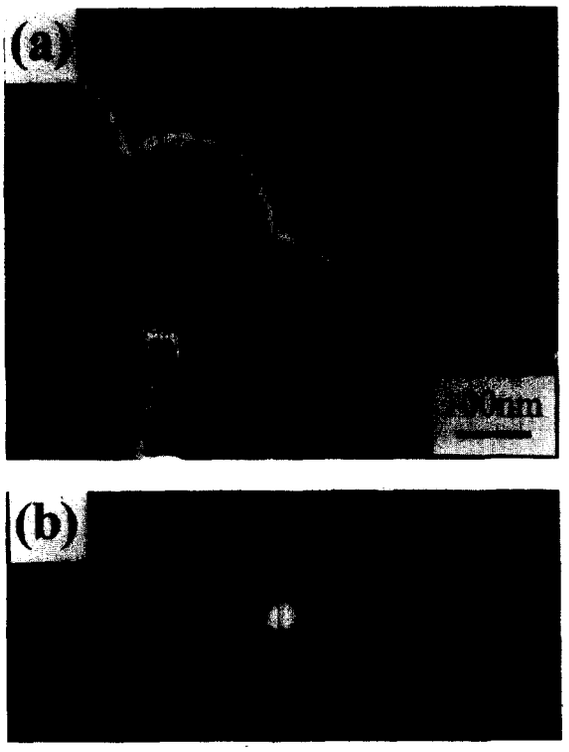

Fig. 12. TEM micrographs of a domain extending across several particles. Tetragonal zirconia calcined in nitrogen at 500°C for 1 h: (a) dark field corresponding to the (202) spot, (b) diffraction pattern.

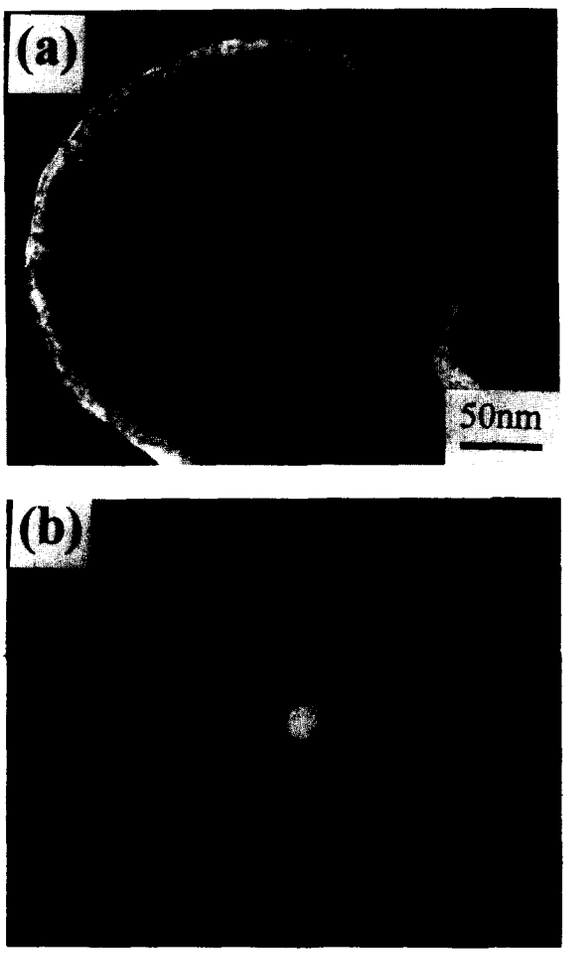

Fig. 13. TEM micrographs of a single domain of monoclinic zirconia. Specimen calcined in air for 1 h at 600°C: (a) dark field image corresponding to the (111) spot, (b) diffraction pattern showing diffuse spots.

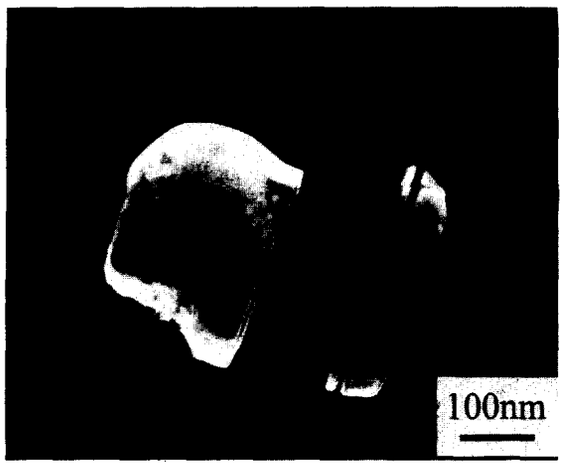

Fig. 14. TEM micrographs of a single domain of monoclinic zirconia exhibiting (100) twinning. Specimen calcined in air for 1 h at 1000°C.

mechanisms by which the nuclei could subsequently grow to micron sized particles, e.g. (a) by the agglomeration of existing nuclei, (b) by the diffusion of molecular species to the surface of existing nuclei, (c) by further nucleation, either continuous or in bursts, during ageing followed by the accretion of the new nuclei onto existing particles, (d) Ostwald ripening, or a mixture of these mechanisms. None of these mechanisms is incompatible with the development of a monodisperse distribution after the initial burst of homogeneous nucleation, nor with a correlation of final particle size with reactant concentration. The growth mechanism will, however, be expected to determine the internal structure and properties of the final particles. In our work, the low density of the spherical particles, even in their calcined state, as evidenced by their transparency in TEM, and their 'grainy' appearance (Figs 11, 12 and 13), seems more consistent with particle growth by the aggregation of particles smaller than 5 nm. Although the precipitate material was essentially amorphous, the packing of the colloidal particles was not necessarily random. Dipole charging of the colloidal particles, for example, could result in an ordered structure. If short-range ordering in the precipitate material was sufficient to induce a structure dependent dipole charging, then a primitive form of long-range ordering might exist. The existence of any primitive form of long-range ordering might later be expected to facilitate crystallization during calcination.

A fully crystalline structure developed at a much lower temperature (300°C) in our homogeneously precipitated material than in any other zirconia precursor so far reported in the literature. The tetragonal phase developed slowly at 300°C and was not associated with a rapid release of bound hydroxyl groups at the 'glow exotherm' temperature of around 450°C which was reported by other authors[20,29–31] as being a prerequisite for crystallization. In our material, a well-defined 'glow exotherm' type of process did occur at 406°C in nitrogen and at 420°C in air, i.e. at least 100°C above the crystallization temperature. Although the lattice parameters of our tetragonal phase changed with temperature, there was no sudden change associated with the 'glow exotherm' process. In fact, most of the change in lattice parameters was due to an increase in the c parameter with increasing temperature, which hardly seems compatible with the loss of species from the lattice. We conclude therefore that if the 'glow exotherm' in our material was due to loss of hydroxyl groups, then these would have been predominantly surface bound groups. An appreciable amount of such bound surface groups could be accommodated on the large internal surface of the highly porous particles. Consequently we attribute the low crystallization temperature to a lack of bound hydroxyl groups within the structure of the precipitate particles at 300°C. We have no evidence to support the existence of an intermediate tetragonal phase with a chemical composition corresponding to $ZrO_{1.5}OH$, as suggested by Aiken *et al.*[6] since we did not find a diffraction peak at $d = 4{\cdot}11$ Å in our material.

The lattice spacings of the tetragonal phase calcined in air differ significantly from that calcined in nitrogen. For a given temperature, c, a, the c/a ratio, and the unit cell volume were all smaller for calcinations in nitrogen than in air. The c/a ratio is a measure of the tetragonality, or the deviation from a cubic system, and it appears that the closer the tetragonal phase approaches to the cubic system, the higher is the stability of the tetragonal phase at elevated temperature. This could be one factor in explaining the higher stability of the tetragonal phase calcined in nitrogen. Microstrain was also lower in nitrogen-calcined material. The reduced lattice spacings in nitrogen may possibly be directly due to the nitrogen atmosphere itself, i.e. to the presence of oxygen vacancies, or to a different level of residual impurities, e.g. anions, compared with air-calcined material. Whereas 90% of the (t → m) transformation in air occurred at about 600°C, there was already a small amount of monoclinic zirconia present in samples calcined in air at 380°C and 500°C which appears to be unrelated to the main (t → m) transformation and which may be the result of a surface (t → m) transformation. We do not attribute this transformation to mechanical handling because similar powder calcined in air at 300°C was 100% tetra-

gonal, as were powders calcined in nitrogen. It seems more likely that a surface (t → m) transformation was induced by the enhanced availability of oxygen and more efficient removal of decomposition products at the particle surface.

Comparing calculated values of apparent crystallite size for planes of the same family indicated the presence of significant amounts of microstrain. The effective crystallite size, calculated from the Hall equation, is a somewhat better indication of crystallite size, although it still underestimates the true geometric crystallite size. The fact that we are dealing with an agglomeration of partially linked particles adds a further complication to the interpretation of these results. The wide range of values for apparent and effective crystallite size in different crystallographic directions therefore cannot be attributed with confidence solely to a non-equiaxed crystallite shape. Moreover, it is doubtful whether it is valid to consider the value for just one set of planes (e.g. the [111] family as frequently quoted in the literature) as characteristic of the material. Nevertheless, it is noteworthy that in all cases the effective size of tetragonal crystallites was larger than the reported critical size[17] to an extent that must be regarded as anomalous and requiring explanation. One possibility is that the effective size that we calculated corresponded to (but underestimated) the size of the domains observed by TEM and that these domains consisted of ordered smaller crystallites instead of being true single crystals. Evidence for such an internal structure to the domains comes from the diffuse nature of the electron diffraction spots which suggests a slight mismatch in the orientation of the crystallites. TEM images showed that domain boundaries were preserved during the (t → m) transition, and the diffuse nature of the diffraction spots of the monoclinic phase suggests that the substructure of slightly misoriented crystallites was also preserved. The detailed microtexture of the domains, however, remains to be investigated.

The tetragonal phase was sub-stoichiometric whether calcined in air or in nitrogen. In air the (t → m) transformation appeared to coincide with the chemisorption of oxygen observed at about 600°C, but in nitrogen, where such an oxygen uptake was excluded, the (t → m) transformation took place at 700°C. This suggests that the metastable tetragonal phase was stabilized by oxygen vacancies.

These findings extend the already wide variety of results reported in the literature regarding the stability of the metastable tetragonal phase prepared under different conditions. The low crystallization temperature, not associated with a 'glow exotherm', the sub-stoichiometry of the tetragonal phase, and the existence of large domains of tetragonal zirconia all emphasize the primary importance of the structure and composition of the quasi-amorphous precipitate in determining the properties of the calcined material.

5 CONCLUSIONS

Zirconia powders consisting of monodisperse spherical particles were prepared by homogeneous precipitation from aqueous solutions of zirconium sulphate plus urea. Particle diameters depended linearly on the initial concentration of $Zr(SO_4)_2$. The spherical particles were probably low density aggregates of colloidal particles of zirconium oxybasic carbonate. The most important characteristics of these particles were (a) the low temperature at which they crystallised to tetragonal zirconia and (b) the large size of the domains in the metastable tetragonal zirconia and the unusual sub-structure of those domains. Crystallization of sub-stoichiometric tetragonal zirconia occurred at temperatures as low as 300°C and the transformation to monoclinic occurred at about 600°C or about 700°C depending on whether the calcination was in air or nitrogen. The low crystallization temperature is attributed to the chemical nature of the precipitate material — specifically to the lack of bound hydroxyl groups within the amorphous structure. The stability of the tetragonal phase appeared to depend on the existence of oxygen vacancies and the resultant low *c/a* ratio. Calcination in nitrogen produced tetragonal zirconia with a lower *c/a* ratio and less microstrain than zirconia calcined in air. The existence of the metastable tetragonal phase in domains of up to about 100 nm diameter is attributed to the existence of a substructure consisting of slightly misoriented and much smaller crystallites that yielded a single crystal electron diffraction pattern with diffuse spots. Both the domain structure and its substructure were preserved during the transition to monoclinic zirconia. We conclude that the most important characteristics of the calcined powder were primarily determined by the structure and composition of the amorphous precipitate from which they were derived.

ACKNOWLEDGEMENTS

B. Djuričić was supported during this work as a visiting scientist by the European Commission. Mr R. Nyquist (ECN, The Netherlands) is thanked for performing the DTA and TG analysis.

REFERENCES

1. CLAUSSEN, N. & RÜEHLE, M., Design of transformation-toughened ceramics, In *Science and Technology of Zirconia I, Advanced Ceramics, Vol. 3*, ed. A. H. Heuer & L. Hobbs. The American Ceramics Society, Columbus, OH, 1981, pp. 137–63.
2. LANGE, F. F., Powder processing science and technology for increased reliability. *J. Am. Ceram. Soc.*, **72** (1989) 3–15.
3. VAN DE GRAAF M. A. C. G. & BURGGRAAF, A. J., Wet-chemical preparation of zirconia powders: Their microstructure and behaviour. In *Science and Technology of Zirconia II, Advanced Ceramics, Vol. 12*, ed. N. Claussen, M. Rühle & H. Heuer.The American Ceramics Society, Columbus, OH, 1983, pp. 744–63.
4. ROOSEN, A. & HAUSNER, H., Sintering kinetics of ZrO_2 Powders. In *Science and Technology of Zirconia II, Advanced Ceramics, Vol. 12*, ed. N. Claussen, M. Rühle & H. Heuer. The American Ceramics Society, Columbus, OH, 1983, pp. 714–26.
5. PAMPUCH, R., ZrO_2 micropowders as model systems for the study of sintering. In *Science and Technology of Zirconia II, Advanced Ceramics, Vol. 12*, ed. N. Claussen, M. Rühle & H. Heuer. The American Ceramics Society, Columbus, OH, 1983, pp. 733–43.
6. AIKEN, B., HSU, W. P. & MATIJEVIĆ, E., Preparation and properties of uniform mixed and coated colloidal particles — Part V: Zirconium Compounds. *J. Mater. Sci.*, **25** (1990) 1886–94.
7. HABERKO, K., Characteristics and sintering behaviour of zirconia ultra fine powder. *Ceramurgia Int.*, **5**(4) (1979) 148–54.
8. DJURIČIĆ, B., KOLAR, D. & KOMAC, M., Synthesis and characteristics of zirconia fine powders from organic zirconium complexes. *J. Mater. Sci.*, **25** (1990) 1132–6.
9. UCHIYAMA, K., OGIHARA, T., IKEMOTO, T., MIZUTANI, N. & KATO, M., Preparation of monodispersed Y-doped ZrO_2 powders. *J. Mater. Sci.*, **22** (1987) 4343–7.
10. MATIJEVIĆ, E., Monodispersed metal (hydrous) oxides — a fascinating field of colloid science. *Acc. Chem. Res.*, **14** (1981) 22–9.
11. MATIJEVIĆ, E., BELL, A., BRACE, R. & MCFADYEN, P., Formation and surface characteristics of hydrous oxide sols. *J. Electrochem. Soc.*, **120** (1973) 893–9.
12. MATIJEVIĆ, E., Production of monodispersed colloidal particles. *Ann. Rev. Mater. Sci.*, **15** (1985) 483–516.
13. AKINC, M. & SORDELET, D., Preparation of yttrium, lanthanum, cerium and neodymium, basic carbonate particles by homogeneous precipitation. *Adv. Ceram. Mater.*, **2** (1987) 232–8.
14. DJURIČIĆ, B., KOLAR, D. & MEMIC, M., Synthesis and properties of Y_2O_3 powder obtained by different methods. *J. Eur. Ceram. Soc.*, **9** (1992) 75–82.
15. DJURIČIĆ, B., MCGARRY, D. & PICKERING, S., Preparation and coating of ultrafine Ce-stabilized ZrO_2 particles with yttria. *J. Mater. Sci. Lett.*, **12** (1993) 1320–3.
16. GOÑI ELIZADE, S. & GARCÍA CLAVEL, M., Characterisation studies of goethite samples of varying crystallinity obtained by the homogeneous precipitation method. *J. Am. Ceram. Soc.*, **73** (1992) 121–6.
17. GARVIE, R. C., Stabilisation of the tetragonal structure in zirconia microcrystals. *J. Phys. Chem.*, **82** (1978) 218–24.
18. OSENDI, M. I., MOYA, S. S., SERNA, J. & SORIA, J., Metastability of tetragonal zirconia powders. *J. Am. Ceram. Soc.*, **68** (1985) 135–9.
19. YAMAGUCHI, T. & TANABE, K., Preparation and characterisation of ZrO_2 and SO_4-promoted ZrO_2. *Mater. Chem. Phys.*, **16** (1986) 67–77.
20. LIVAGE, J., DOI, K. & MAZIERES, C., Nature and thermal evolution of amorphous hydrated zirconium oxide. *J. Am. Ceram. Soc.*, **51** (1968) 349–53.
21. TANI, E., YOSHIMURA, M. & SOMIA, S., Formation of ultrafine tetragonal ZrO_2 powder under hypothermal conditions. *J. Am. Ceram. Soc.*, **66** (1983) 11–4.
22. MURASE, Y. & KATO, E., Role of water vapour in crystallite growth and tetragonal–monoclinic phase transformation of ZrO_2. *J. Am. Ceram. Soc.*, **66** (1983) 196–200.
23. MITUHASHI, T., ICHIHARA, M. & TATSUKE, U., Characterisation and stabilisation of metastable tetragonal ZrO_2. *J. Am. Ceram. Soc.*, **57** (1974) 97–101.
24. MERCERA, P. D. L., VAN OMMEN, J. G., DOESBURG, E. B. M., BURGGRAAF, A. J. & ROOS, J. R. H., Influence of ethanol washing of the hydrous precursor on the textural and structural properties of zirconia. *J. Mater. Sci.*, **27** (1992) 4890–98.
25. SHAW, W. H. R. & BORDEAUX, J. J., The decomposition of urea in aqueous media *J. Am. Ceram. Soc.*, **77** (1955) 4729–33.
26. TORAYA, H., YOSIMURA, M. & SOMIA, S., Calibration curve for quantitative analysis of the monoclinic–tetragonal ZrO_2 system by X-ray diffraction. *J. Am. Ceram. Soc.*, **67** (1984) C119–C21.
27. KLUG, H. P. & ALEXANDER, L. E., *X-ray Diffraction Procedures*. Wiley, New York, 1954, pp. 618–703.
28. ITOCH, T., Particle and crystallite sizes of ZrO_2 powder obtained by the calcination of hydrous zirconia. *J. Mater. Sci. Lett.*, **4** (1985) 431–3.
29. GIMBLET, G., RAHMAN, A. A. & SING, K. S. W., Thermal and related studies of some zirconia gels. *J. Chem. Tech. Biotechnol.*, **30** (1980) 51–64.
30. MERCERA, P. D. L., VAN OMMEN, J. G., DOESBURG, E. B. M., BURGGRAAF, A. J. & ROOS, J. R. H., Zirconia as a support for catalysts — evolution of the texture and structure on calcination in air. *Appl. Catal.*, **57** (1990) 127–48.
31. SRINIVASAN, R., HARRIS, M. B., SIMPSON, S. F., DEANGELIS, R. J. & DAVIS, B. H., Zirconium oxide crystal phase: The role of the pH and time to the attain of the final pH for precipitation of the hydrous Oxide. *J. Mater. Res.*, **3** (1988) 787–97.
32. TORRALVO, M. J., ALARIO, M. A. &. SORIA, J., Crystallisation behaviour of zirconium oxide gels. *J. Catal.*, **86** (1984) 473–6.
33. WEBB, T. L. & KRUEGER, J. E., *Thermal Analysis*, ed. R. C. Mackenzie. Academic Press, New York, 1979, pp. 302–41.
34. KALISZEWSKI, M. S. & HEUER, A., Alcohol interaction with zirconia. *J. Am. Ceram. Soc.*, **73** (1990) 1504–9.
35. WEN, T. L., HEBERT, W., VILMINOT, S. & BERNIER, J. C., Preparation of nanosized yttria-stabilized zirconia powders and their characterisation. *J. Mater. Sci.*, **26** (1991) 3787–91.
36. TURRILAS, X., BERNES, P., HAEUSERMANN, D., JONES, S. L. & NORMAN, C. J., Effect of chemical and heat treatment on the tetragonal to monoclinic transformation of zirconia. *J. Mater. Res.*, **8** (1993) 163–8.
37. SRINIVASAN, R., DAVIS, B. H., BURLCAVIN, O. & HUBBARD, C. R., Crystallisation and phase transformation process in zirconia: an *in-situ* high-temperature X-ray diffraction study. *J. Am. Ceram. Soc.*, **75** (1992) 1217–22.